The galaxy alignment effect in Abell 1689: evolution, radial and luminosity dependence

Li-Wei Hung[1], Eduardo Bañados[2], Roberto De Propris[3], Michael J. West[4]

Received _____; accepted _____

[1]Department of Astronomy, Ohio State University, Columbus, OH, USA

[2]Departamento de Astronomia y Astrofisica, Pontificia Universidad Catolica, Santiago, Chile

[3]Cerro Tololo Inter-American Observatory, La Serena, Chile

[4]European Southern Observatory, Santiago, Chile

ABSTRACT

We measure alignments on scales of 1 Mpc h_{71}^{-1} for galaxies in Abell 1689 ($z = 0.18$) from an existing Hubble Space Telescope mosaic. We find evidence of galaxy alignment in the inner 500 h_{71}^{-1} kpc. The alignment appears to be stronger towards the centre and is mostly present among the fainter galaxies, while bright galaxies are unaligned. This is consistent with a model where alignments originate from tidal locking.

Subject headings: galaxies: clusters: individual: Abell 1689

1. Introduction

Alignments between galaxies and their host structures is predicted to occur in ΛCDM models (e.g., Faltenbacher et al. 2005; Hopkins, Bahcall & Bode 2005; Basilakos et al. 2006). For instance, in turbulence models, galaxies' major axes should align with the major axis of the closest large scale structure (Shandarin 1974; Efstathiou & Silk 1983), while Navarro, Abadi & Steinmetz (2004) relate the alignment of spiral galaxies to the acquisition of angular momentum via tidal torques.

Perhaps the best known example of preferential galaxy alignments is the observation that the major axis of brightest cluster galaxies (BCGs) is oriented along the distribution of cluster members and 'points' towards other nearby clusters on scales of $\sim 10 - 20$ Mpc h^{-1} (e.g., Binggeli 1982; Struble 1990; Trevese, Cirimele & Flin 1992; Fuller, West & Bridges 1999; Niederste-Ostholt et al. 2010 among others). This is explained by the formation of BCGs via a process of collimated infall along filaments feeding the cluster growth (West 1994; Dubinski 1998).

It is unclear whether other cluster galaxies other than the BCGs are expected to show preferential alignments (direct alignments with the BCG axis) in CDM models (e.g., West, Villumsen & Dekel 1991). Any primordial alignments may not survive the cluster environment, as they are erased by strong dynamical interactions (Coutts 1996; Plionis et al. 2003). On the other hand, the cluster tidal field may eventually induce new alignments by a process of tidal locking akin to the Earth-Moon system (Ciotti & Dutta 1994, Pereira, Bryan & Gill 2008).

Direct galaxy alignments have been detected for some clusters (Plionis et al. 2003; Aryal & Saurer 2006) but not in others (Strazzullo et al. 2005; Aryal, Kandel & Saurer 2006). It is likely that the alignments depend on mass, cluster age and position in complex ways. Arguably, the best studied example is the Coma cluster. In a comprehensive study

using high quality multi-color imaging and spectroscopy, Torlina, De Propris & West (2007) found no evidence of preferential alignments other than for the two brightest cluster members for the inner 400 h^{-1} kpc of the Coma cluster. Adami et al. (2009a) broadly confirm this result but find some evidence of alignment for the fainter cluster members and in areas that appear to coincide with substructure. Plionis et al. (2003) detect a clear alignment signal in Abell 521, but this is a dynamically young object containing rich substructures and the alignment appears to correlate with the individual subclusters.

The evolution of the alignment effect offers clues to its origin and possibly constraints on galaxy formation models and their interaction with large scale structure. We may expect that higher redshift clusters, observed closer to the epoch of their formation, may yield a stronger signal if primordial alignments are important. In the models of Pereira et al. (2008) initial alignments are quickly destroyed, but the direct alignment increases with time because of tidal torques. Niederste-Ostholt et al. (2010) have studied the alignment of BCGs with their clusters at $0 < z < 0.4$ and found that more dominant central galaxies are more strongly aligned and that the effect is stronger at lower redshifts, a result that can be interpreted within the framework of hierarchical accretion and growth.

In this paper we study the alignment effect in Abell 1689 over a ~ 1 Mpc h^{-1} field from a wide mosaic of Hubble Space Telescope (HST) data. This is the most distant cluster where the alignment effect has been searched for. HST observations provide the necessary spatial resolution and stable point spread function necessary to measure the position angles and ellipticities of faint galaxies at high redshift. We describe the data and analysis in section 2. The results are reported in section 3 and discussed in section 4. We adopt the latest WMAP7 cosmological parameters: $\Omega_M = 0.27$, $\Omega_\Lambda = 0.73$ and $\mathrm{H}_0 = 71$ km s^{-1} Mpc^{-1}.

2. Data and Analysis

The data used in this project consist of a 4×4 mosaic of WFPC2 (Wide Field and Planetary Camera 2) images covering a total of $10'$ on the side (PID: 5993; PI: Kaiser). Exposure times were 1800s in V (F606W) and 2300s in I (F814W). All data were retrieved as fully processed images from the Hubble Legacy Archive website.

Photometry for objects in these fields was carried out using Sextractor (Bertin & Arnouts 1996). Further details about the photometry may be found in a companion paper by Bañados et al. (2010, submitted) dealing with the galaxy luminosity function in Abell 1689, but we summarize the most relevant points here. Sextractor was run twice, once with parameters appropriate to the detection and photometry of bright galaxies, without excessively deblending their images, and then with parameters suited to faint galaxies. The same parameters as in Leauthaud et al. (2007) were used. This allowed us (see Bañados et al. for details) to use the COSMOS counts to statistically subtract the fore/background contribution to determine the cluster LF.

We selected galaxies in the I band, both because this is the COSMOS selection band and because this is better related to the stellar mass. However, we also measure two aperture magnitudes in V and I, to derive galaxy colors and use these to identify a sample of cluster members via their position with respect to the cluster red sequence (see below). We also measure, for each galaxy, its ellipticity and position angle. We use the values determined from the I band, but we find that the values from the V band images are identical to within a few % (Figure 1). All images were visually inspected to remove spurious objects, satellite trails and (especially) arclets. Magnitudes were calibrated on to the AB system with tabulated zeropoints.

In order to use these data for the alignment effect we need to isolate a sample of cluster members. Lacking a large redshift survey or numerous bands to measure photometric

redshifts, we use galaxies on the color-magnitude relation as these are likely to consist predominantly of cluster members. We plot the $V - I$ vs. I color-magnitude diagram of galaxies in Abell 1689 in Figure 2, where we assume that galaxies within ± 0.3 mag. of the color-magnitude defined by the brighter galaxies are cluster members. The faint-end limit of our selection is set by our ability to carry out star-galaxy separation (see Bañados et al. 2010, their Figure 1). Note that the red sequence LF in Bañados et al. is in very good agreement with their total LF, arguing that most cluster members indeed lie on the red sequence. However, this selection limits the sample of objects to E/S0 galaxies and dwarf 'ellipticals'; some galaxies in the blue cloud may be cluster members, but we have no way of determining membership, other than by the red sequence, and including them in our study, with present data.

In Coma, Adami et al. (2009b) find that the scatter on the red sequence increases for $M_R > -18$, while in Virgo (Janz & Lisker 2008) find an increase in the scatter at $M_R > -14$; we instead use a rectangular aperture around the best fit to the color-magnitude relation to select members. However, we choose to be conservative in our selection, as enlarging the color 'box' used in Figure 2 runs the risk of including an increasing fraction of non-cluster members, especially at the faint end where the field counts are increasing steeply, and where color errors become more significant (preferentially scattering blue galaxies on to the red sequence), and therefore potentially diluting the sample. This might indeed be an issue in the cluster outskirts, where the relative fraction of cluster members decreases rapidly.

As shown by Holden et al. (2009) we need to be careful to understand the limits of our method to obtain reliable measurements of the galaxy position angle. This depends on the spatial resolution of the image, the point spread function and the ellipticity of galaxies (round objects have no real orientation, of course). In order to do this, we carry out a series

of simulations, by placing artificial images with $17 < I < 25$ (the approximate star/galaxy separation limits in Banados et al. 2010), $0.0 < e < 0.7$ and random position angles, using the IRAF/ARTDATA package. We proceed to detect these galaxies in the same fashion as our targets and measure how the ellipticity and position angle are recovered as a function of input ellipticity and apparent magnitudes. All the images were convolved with a Gaussian having appropriate FWHM for HST images. We used the size-luminosity relation for Virgo galaxies by Janz & Lisker (2008) to derive input sizes as a function of magnitude, using de Vaucoleurs profiles for galaxies brighter than $M_I = -18$ and exponential profiles for fainter ones. A total of 100 galaxies per magnitude (in 1 mag. interval) and ellipticity (in 0.05 intervals) steps were simulated, for a total of 14,000 objects.

The results of this exercise are shown in Figures 3 and 4, plotting Δe (input minus output) vs. I as a function of input e and Δ PA vs. I, also as a function of input e. Based on these plots, we choose to trust only galaxies for which we can determine e to within 0.1 and the PA to 20°. Targets for our study are therefore galaxies with $I < 24$, $e > 0.2$ and lying on the red sequence in Figure 2.

3. The alignment effect in Abell 1689

Figure 5 (upper panel) shows the PAs of all galaxies used across the cluster field, plotted as a segment. The brightest cluster galaxy is identified as a thick red segment. The middle panel shows a histogram of the distribution of position angles, while the bottom panel presents the results of a Kuiper test, to determine whether there is alignment and its significance (cf., Torlina et al. 2007).

According to this test, there is a marginal $\sim 1.5\sigma$ detection of alignment in this cluster. If alignment exists, we are also interested in whether this is primordial or newly induced by

tidal interactions. In the models by Pereira et al. (2008) the alignment signal should rise towards the cluster centre but drop again closest to the BCC, while Aragon-Calvo et al. (2007) detected a weak primordial alignment signal by stacking several hundred clusters from the SDSS (in comparison, Torlina et al. 2007 find no alignment along the filaments surrounding the Coma cluster).

We plot the histogram of PAs and the Kuiper test results for regions within 0 – 200 kpc (projected) from the cluster centre, 200 – 400 kpc, 400 – 600 kpc and 600 – 1000 kpc, in Figure 6 (with cosmology as indicated above). The results are that there is relatively significant alignment (P values of about 0.12 or about 2σ) in the two inner regions, but no detection in the two outer ones. In addition, the PA of the maximum deviation from uniformity is $\sim 30^\circ$ – 60° in both the two inner regions and this is also very close to the measured PA of the brighter cluster galaxy (26°), arguing that the measured alignment is likely to be real and to consist of direct alignment between galaxies and the BCG. However, the lack of alignment signal in the outer regions may at least partly be due to the increased degree of contamination from field galaxies.

As a test, we also consider the distribution of the acute angles between the galaxy PAs and the great circle connecting each galaxy to the cluster centre and find no evidence of a radial alignment (with galaxies pointing to the cluster centre as in Pereira & Kuhn 2005). We therefore conclude that we find evidence of so-called direct alignment where galaxies point along the major axis of the cluster distribution and the BCG.

We may further ask what galaxies are responsible for the observed signal. In Figure 7 we plot the histogram of PAs and Kuiper test for bright ($M_I < -18$) and faint ($M_I > -18$) galaxies. The bright galaxies are not aligned, in good agreement with the Coma data of Torlina et al. (2007), but the faint galaxies show significant (better than 2σ) alignment, with PA consistent with that measured in Figure 5. We infer from this that the alignment

we measure is due to a population of fainter galaxies residing prevalently in the cluster centre.

While the giant galaxies are not aligned, we may also ask whether there is an aligned component. We can only classify galaxies into E or S0, because of our color selection. For these objects, Figure 8 shows the results of the Kuiper test. There is no evidence of alignment among the giant galaxies, irrespective of morphology.

4. Discussion

Our results show evidence of an alignment signal in the inner region of Abell 1689 and also imply that while bright galaxies are not aligned, the fainter galaxies are responsible for most of the observed signal, at least in Abell 1689. The results for bright galaxies are in agreement with the work in Coma by Torlina et al. (2007), while the stronger alignment for fainter galaxies is at least partially consistent with Adami et al. (2009a).

The most comprehensive theoretical study of the alignment effect come from Pereira et al. (2008). Based on a series of N-body simulations in a ΛCDM universe, Pereira et al. (2008) find that the alignment effect is independent of cluster mass, that there is a degree of primordial alignment at large radii and the alignment becomes stronger towards the cluster centre, owing to tidal forces, while its strength should grow with decreasing redshift. The work by Plionis et al. (2003) argues that the alignment is stronger for dynamically young clusters, where galaxies still 'preserve' the memory of their infall history.

Our results are in broad agreement with some of these predictions. We detect no alignment in the outskirts, although the signal may be too weak for us to detect (Aragon-Calvo et al. 2007). In the cluster outskirts, contamination of the sample by non

members would tend to dilute any alignment as well. In agreement with the expectations from theory, the alignment signal becomes stronger towards the cluster centre. The model by Pereira et al. (2008) makes no strong predictions concerning the size of the alignment effect as a function of satellite mass. In our case, the bright galaxies show no significant signal, as they do in Coma (Torlina et al. 2007). This is true even when we separate E from S0. Even in a sample of above 300 clusters at low redshift, Pereira & Kuhn (2005) find only a weak signal. This is partly due to the difficulty of measuring the alignment of real stellar distributions as opposed to cleanly defined dark matter halos. However, the alignment effect for giants tends to be much weaker than expected, even in younger clusters. This suggest that there is either no primordial alignment, or that giants have dwelled in cluster environments long enough for any original anisotropy to be erased, while the processes that lead to alignments are either inefficient or have not had sufficient time to operate on the scales of luminous galaxies.

Fainter galaxies are instead significantly aligned, especially in the centre. This is consistent with the tidal model. For brighter galaxies, the change in position angle would take place slowly, over multiple orbits, and would be most effective for radial orbits (Pereira et al. 2008). Thus it is possibly not fully surprising if we detect no alignment signal. On the other hand, we might expect that fainter galaxies will be more strongly affected by the cluster tidal field and would tend to align themselves more rapidly, by analogy with the tidal locking process studied by Ciotti & Dutta (1994).

It is clear that detection of galaxy alignments is difficult: it requires large statistics, high resolution wide-field imaging to measure position angles reliably and either redshift information or colors to select members. Nevertheless, the alignment effect provides a useful test of models for galaxy formation and dynamical evolution. The rich sample of clusters to be gathered by the Multi-Cycle Treasury survey will provide us with a useful dataset to

test this issue further.

Based on observations made with the NASA/ESA Hubble Space Telescope, and obtained from the Hubble Legacy Archive, which is a collaboration between the Space Telescope Science Institute (STScI/NASA), the Space Telescope European Coordinating Facility (ST-ECF/ESA) and the Canadian Astronomy Data Centre (CADC/NRC/CSA).

Facilities: HST (WFPC2).

REFERENCES

Adami, C., Gavazzi, R., Cuillandre, J. C., Durret, F., Ilbert, O., Mazure, A., Pello, R. & Ulmer, M. P. 2009a, A&A, 493, 399

Adami, C., et al. 2009b, A&A, 507, 1225

Aragon-Calvo, M. A., van de Weygaert, R., Jones, B. J. T. & van der Hulst, J. M. 2007, ApJ, 655, L5

Aryal, B. & Saurer, W. 2006, MNRAS, 366, 438

Aryal, B., Kandel, S. M. & Saurer, W. 2006, A&A, 458, 357

Basilakos, S., Plionis, M., Yepes, G., Gottlober, S. & Turchaninov, V. 2006, MNRAS, 365, 539

Bertin, E. & Arnouts, S. 1996, A&AS, 117, 383

Binggeli, B. 1982, A&A, 107, 338

Ciotti, L. & Dutta, S. N. 1994, MNRAS, 270, 390

Coutts, A. 1996, MNRAS, 278, 87

Dubinski, J. 1998, ApJ, 502, 141

Efstathiou, G. & Silk, J. 1983, Fundamentals of Cosmic Physics, 9, 1

Faltenbacher, A., Allgood, B., Gottlober, S., Yepes, G. & Hoffman, Y. 2005, MNRAS, 362, 1099

Fuller, T. M., West, M. J. & Bridges, T. J. 1999, ApJ, 519, 22

Holden, B. P. et al. 2009, ApJ, 693, 617

Hopkins, P. F., Bahcall, N. A. & Bode, P. 2005, ApJ, 618, 1

Janz, J. & Lisker, T. 2008, ApJ, 689, L25

Leauthaud, A. et al. 2007, ApJS, 172, 219

Navarro, J. F., Abadi, M. G. & Steinmetz, M. 2004, ApJ, 613, L41

Niederste-Ostholt, M., Strauss, M. A., Dong, F., Koester, B. P. & McKay, T. A. 2010, astro-ph, 1003.0322

Pereira, M. J. & Kuhn, J. R. 2005, ApJ, 627, L21

Pereira, M. J., Bryan, G. L. & Gill, S. P. D. 2008, ApJ, 672, 825

Plionis, M., Benoist, C., Maurogordato, S., Ferrari, C. & Basilakos, S. 2003, ApJ, 594, 144

Shandarin, S. 1974, Soviet Astronomy, 18, 392

Strazzullo, V., Paolillo, M., Longo, G., Puddu, E., Djorgovski, S. G., de Carvalho, R. R. & Gal, R. R. 2005, MNRAS, 359, 191

Struble, M. F. 1990, AJ, 99, 743

Torlina, L., De Propris, R. & West, M. J. 2007, ApJ, 660, L97

Trevese, D., Cirimele, G. & Flin, P. 1992, AJ, 104, 935

West, M. J., Villumsen, J. V. & Dekel, A. 1991, ApJ, 369, 287

West, M. J. 1994, MNRAS, 268, 79

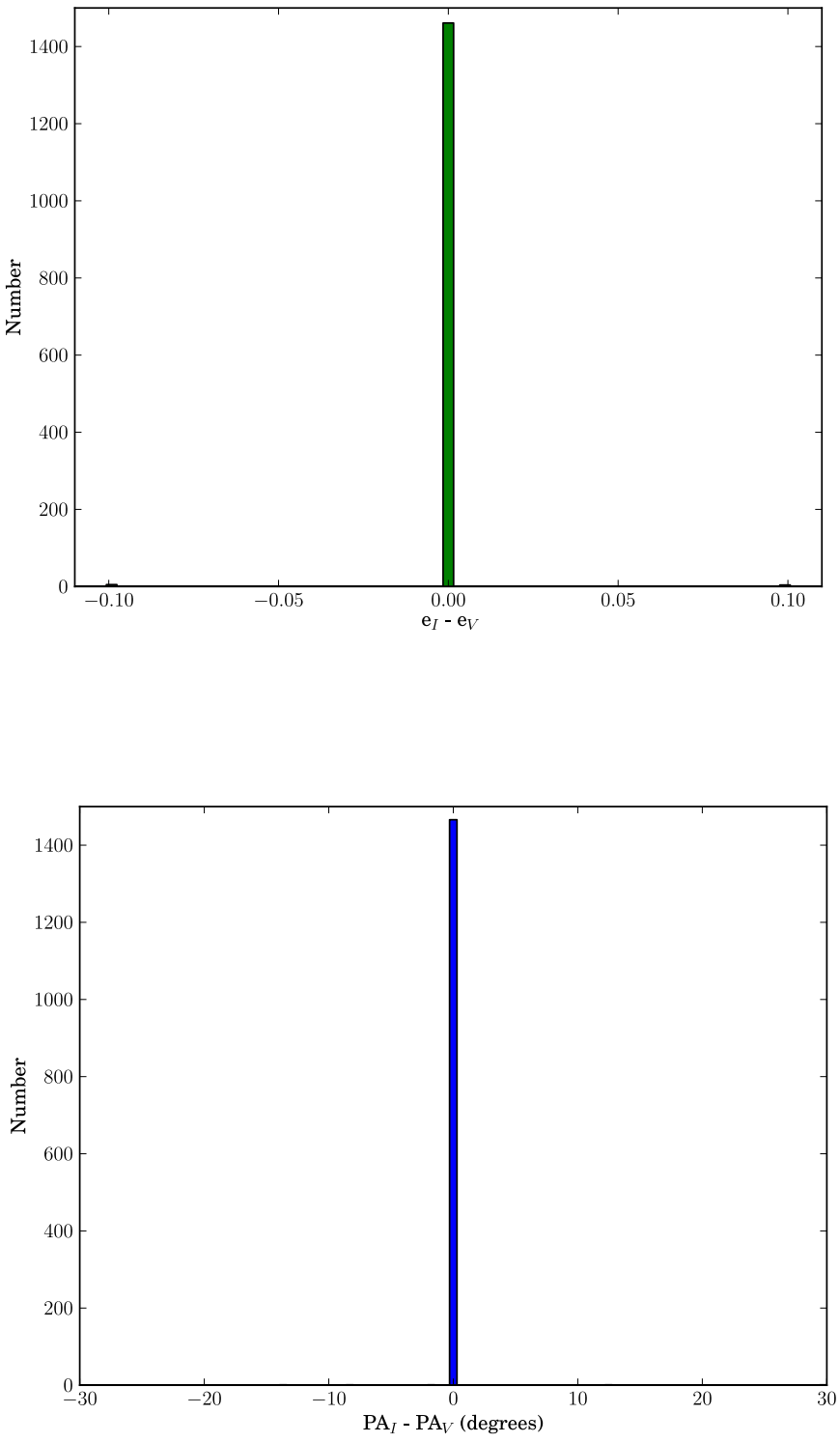

Fig. 1.— Histograms of the difference between ellipticities and position angles as determined from the V and I band images. The mean is zero with a scatter of a few % at most

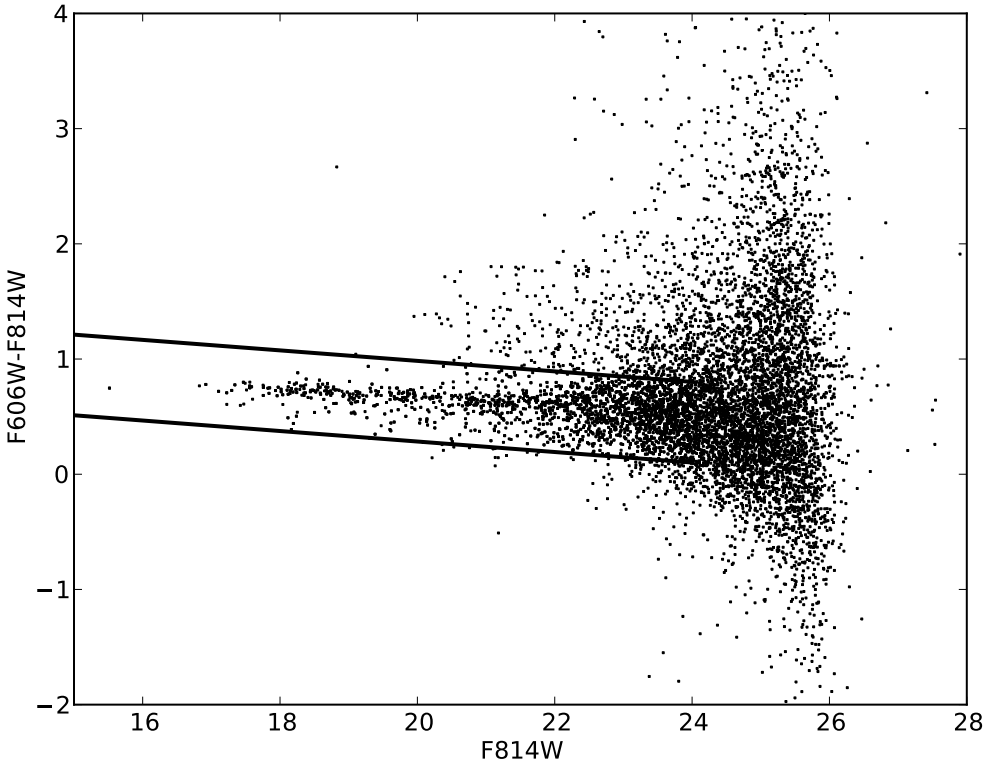

Fig. 2.— Color-magnitude relations in $V - I$ for A1689. We overplot the selection range in color and magnitude that we adopt for membership in the cluster.

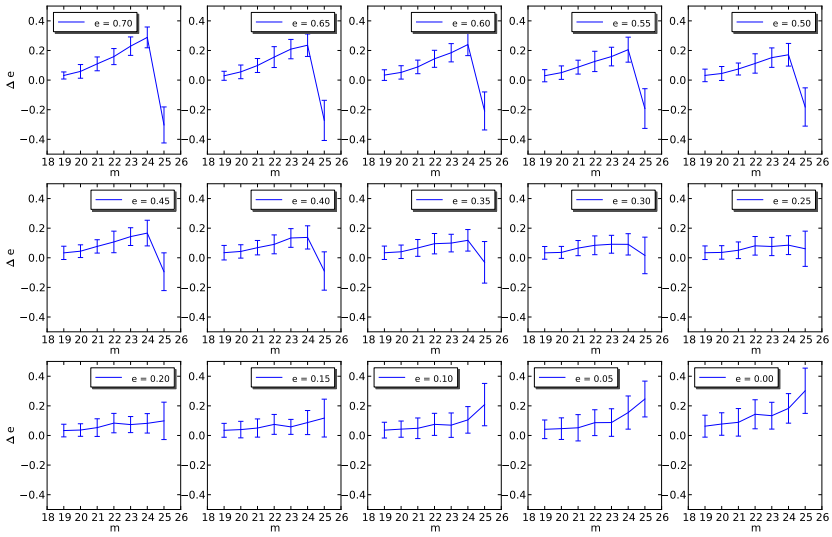

Fig. 3.— Difference between input ellipticity and ellipticity output by Sextractor for simulated galaxies as a function of I magnitude. Each panel corresponds to a different ellipticity identified in the legend.

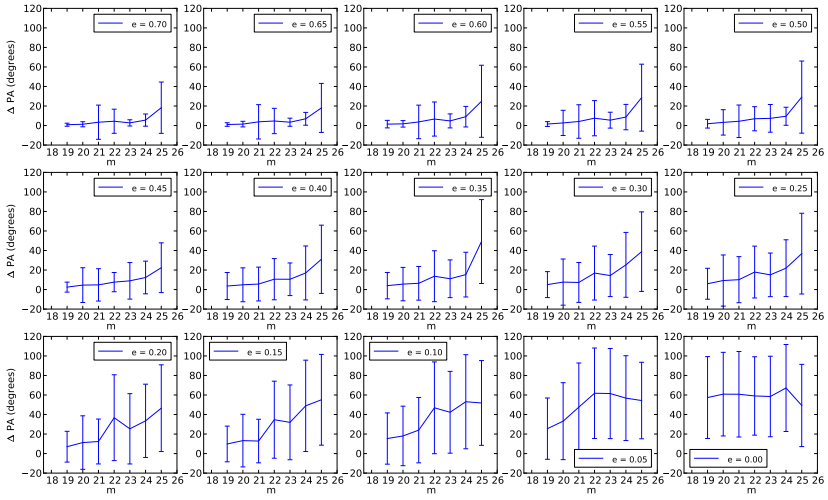

Fig. 4.— Same as Figure 2 but for the difference between input position angle and PA output by Sextractor for simulated galaxies as a function of I magnitude.

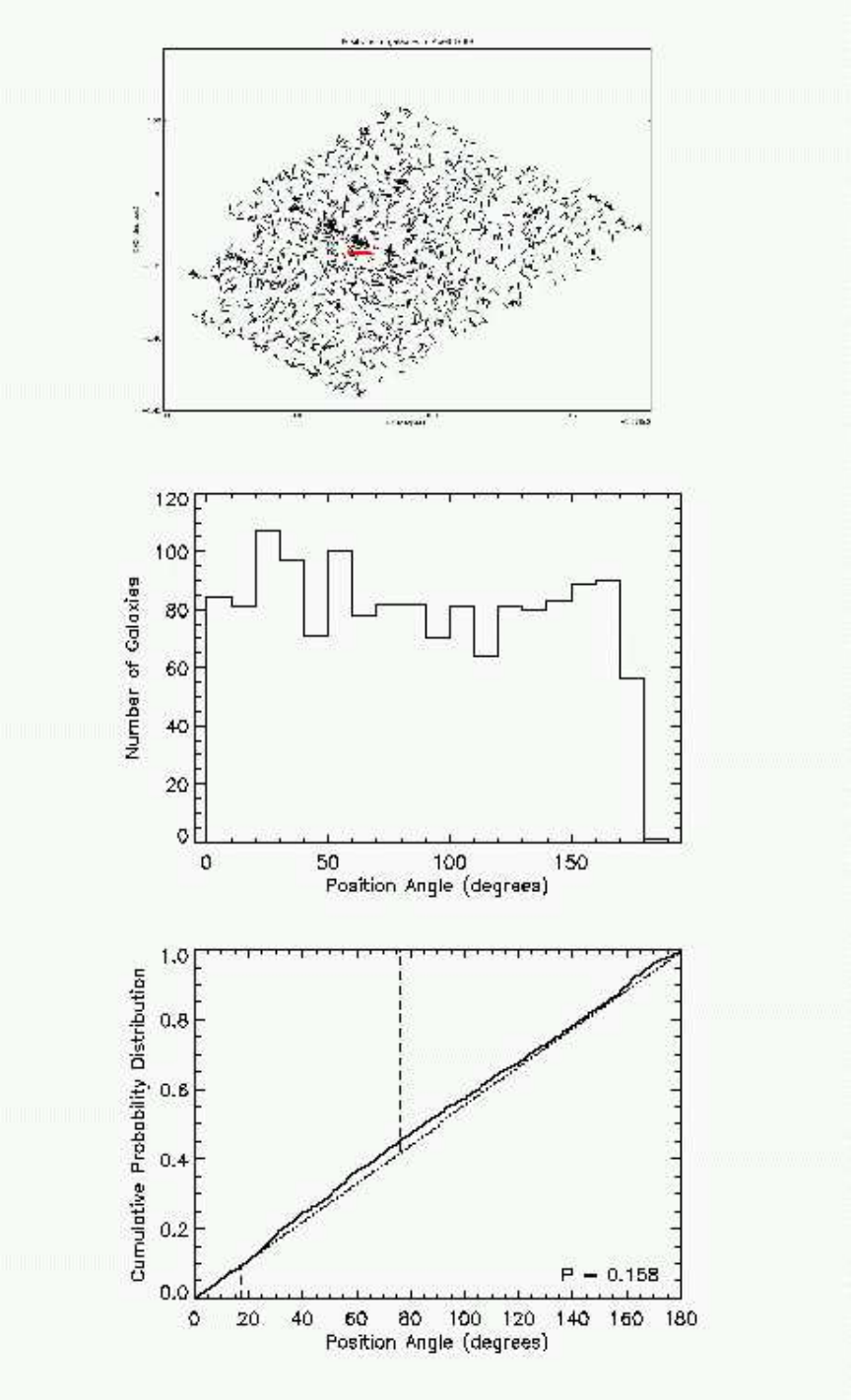

Fig. 5.— *Top panel:* Position angles of Abell 1689 galaxies, with the brightest cluster galaxy marked in red. *Middle panel:* Histogram of position angles. *Bottom panel:* cumulative distribution function compared to a uniform distribution. The P value returned by the Kuiper test is indicated in the figure, as well as the angle of maximum deviation. A lower P value indicates greater alignment.

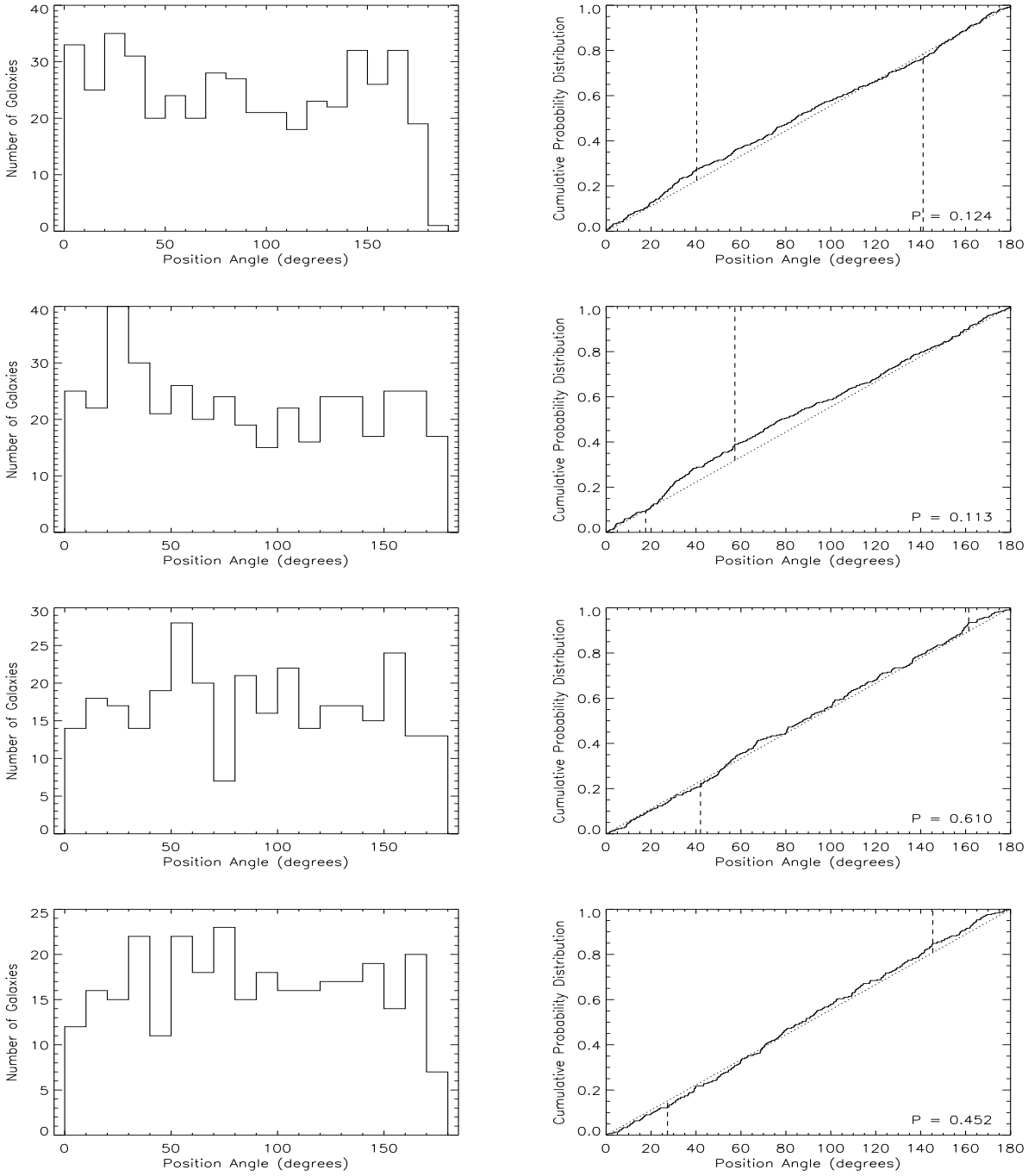

Fig. 6.— Histograms of position angles and probability distributions, with P value from the Kuiper test, placed side-by-side, for galaxies in the 0 – 200 kpc bin from the centre of Abell 1689 (first from top), 200 – 400 kpc (second), 400 – 600 kpc (third) and 600 – 1000 kpc (bottom). Alignment is detected for the first two bins (closer to the centre of the cluster) but not in the outer two.

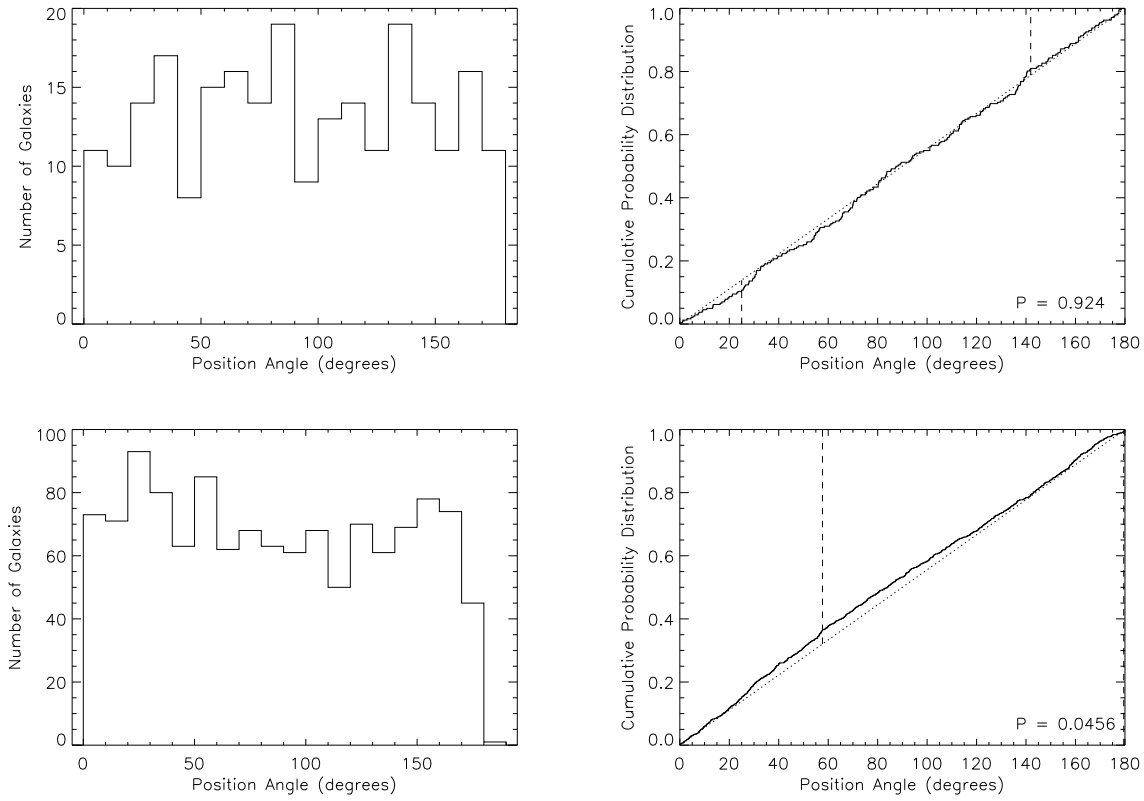

Fig. 7.— Histograms of position angles and probability distributions, with P value from the Kuiper test, for galaxies brighter (top panels) and fainter (bottom) than $M_I = -18$ in Abell 1689.

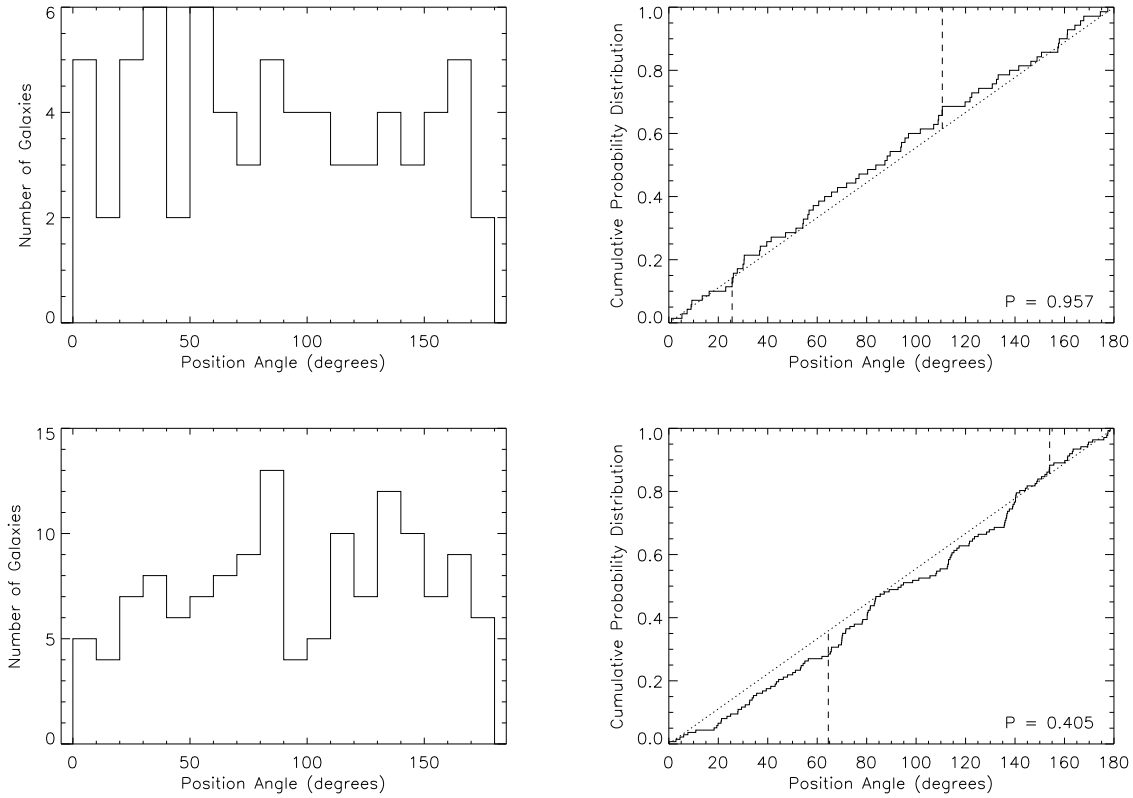

Fig. 8.— Histograms of position angles and probability distributions, with P value from the Kuiper test, for bright galaxies: Ellipticals in the top two panels and S0s in the bottom two panels.